Atmos. Chem. Phys., 25, 10215–10228, 2025
https://doi.org/10.5194/acp-25-10215-2025


Atmospheric Chemistry and Physics
Open Access
EGU



# Carbonate content and stable isotopic composition of atmospheric aerosol carbon in the Canadian High Arctic

**Petr Vodička[1,2], Kimitaka Kawamura[2], Bhagawati Kunwar[2,3], Lin Huang[4], Dhananjay Kumar[2,a], Md. Mozammel Haque[2,5], Ambarish Pokhrel[2], Sangeeta Sharma[4], and Leonard Barrie[6]**

[1]Institute of Chemical Process Fundamentals, Czech Academy of Sciences, 165 00 Prague 6, Czech Republic
[2]Chubu Institute for Advanced Studies, Chubu University, 1200 Matsumoto-cho, Kasugai 487–8501, Japan
[3]Institute for Space-Earth Environmental Research, Nagoya University, Nagoya 464-8601, Japan
[4]Environment and Climate Change Canada, Science and Technology Branch, 4905 Dufferin St., Toronto, Canada
[5]School of Ecology and Applied Meteorology, NUIST, Nanjing, 210044, China
[6]Atmospheric and Oceanic Sciences Department, McGill University, Montreal, Quebec, H3A 0B9, Canada
[a]now at: Commission for Air Quality Management in National Capital Region and Adjoining Areas, New Delhi 110001, India

**Correspondence:** Petr Vodička (vodicka@icpf.cas.cz) and Kimitaka Kawamura (kkawamura@fsc.chubu.ac.jp)

Received: 22 November 2024 – Discussion started: 13 January 2025
Revised: 27 May 2025 – Accepted: 29 June 2025 – Published: 10 September 2025

**Abstract.** The carbon cycle in the Arctic atmosphere is important in understanding abrupt climate changes occurring in this region; 2 years of measurements (summer 2016 to spring 2018) of carbonaceous aerosols at the High Arctic station Alert, Canada, showed that, in addition to organic carbon (OC) and elemental carbon (EC), carbonate carbon (CC) was episodically but not negligibly present. The relative abundances of CC in total carbon (TC) ranged from 0 % to 65 %, with an average of approximately 11 % over the entire period. Also, there was a strong correlation of CC with aerosol $Ca^{2+}$, which is associated mostly with soil dust and, to a lesser extent, sea salt aerosol. Based on this and the analysis of air mass back trajectories (AMBTs), we infer two possible sources of CC in the Arctic total suspended particles (TSPs). The major one is the erosion and resuspension of limestone sediments, particularly in the semi-desert areas of the northern Canadian Arctic. Another potential minor source of CC is marine aerosol, including calcified marine phytoplankton shells (coccoliths) introduced into the atmosphere via sea-to-air emission.

The CC content significantly influenced the stable carbon isotopic composition ($\delta^{13}C$) of TC. The higher the CC content, the higher the $\delta^{13}C$ values, which is consistent with the strong $^{13}C$ enrichment in carbonates. Therefore, carbonates in Arctic TSPs must be taken into account not only in isotopic studies using $\delta^{13}C$ analyses but also when assessing the impact of carbonaceous aerosols on the Arctic climate.

## 1 Introduction

The Arctic is a dynamically changing region that is significantly affected by climate change (England et al., 2021). Aerosols are one of the factors influencing the climate, but their effects are subject to significant uncertainties (Carslaw et al., 2013). The uncertainties in radiative forcing are primarily associated with carbonaceous aerosols, mostly composed of organic carbon (OC). In contrast, a smaller fraction consists of elemental carbon (EC), which is equivalent to optically determined black carbon (BC) (Petzold et al., 2013).

Organic aerosols, i.e., OC in the atmosphere, generally have a cooling effect on the climate (Stjern et al., 2016), except for the part called brown carbon (Laskin et al., 2015). On

the other hand, EC or BC has a warming effect, both in the atmosphere (Liu et al., 2020) and on snow surfaces (Flanner et al., 2007), especially important in the Arctic. In addition, EC and BC measurements are also used to determine the mass absorption cross-section (MAC), a fundamental input to radiative transfer models (Mbengue et al., 2021). The MAC is season- and station-specific (Savadkoohi et al., 2024), making it one of the parameters affecting the influence of aerosols on climate. If either EC or BC is determined inaccurately, the MAC factor will be subsequently biased as well (Chen et al., 2021). Therefore, detailed knowledge of the composition of carbonaceous aerosol in the Arctic is crucial for improving our understanding of their impacts on the climate changes in this region.

Recent atmospheric studies from Tajikistan (Chen et al., 2021) and Tibet (Hu et al., 2023) indicate a significant contribution of carbonates in total suspended particles (TSPs), which may have a significant effect on the determination of OC and EC (or BC). Those areas are characterized as arid desert regions with sparse vegetation, large amounts of unconsolidated sediments, and a lack of soil moisture, with wind erosion playing an important role in the aeolian processes such as atmospheric transport and dust deposits. Arctic regions are affected by long-range transport of dust and also receive contributions of dust locally (Groot Zwaaftink et al., 2016; Sharma et al., 2019; Sirois and Barrie, 1999). They have a desert, semi-desert, or arid character in some cases (Pushkareva et al., 2016). Recently high-latitude dust sources have been described as a significant climate and environmental factor (Kawai et al., 2023; Kawamura et al., 1996; Meinander et al., 2022). It is reported that carbonate-rich dust also has a slightly positive effect on radiative forcing, although this is lower than that of BC (Chen et al., 2021; Raman et al., 2011). High Arctic semi-desert aerosols have been described as potentially important reservoirs of soil organic matter (Muller et al., 2022); however, the influence of carbonates on the atmosphere in these regions has not yet been systematically studied. Investigation of the ion balance of November to May fresh snowfall at the Arctic site Alert over a 3-year period (Toom-Sauntry and Barrie, 2002) led to the conclusion that missing carbonate (especially in November and May) is the most likely cause of the ion imbalance. In addition to dust, it is hypothesized that a source of carbonates in summer Arctic aerosols may be marine microorganisms from sea spray, as reported by Mukherjee et al. (2020) based on calcium analyses.

In recent years, carbon in aerosols has also been subject to analyses of the stable isotopic composition ($\delta^{13}$C) as a method for studying atmospheric processes (Gensch et al., 2014; Huang et al., 2006). Several studies within the Arctic have also employed $\delta^{13}$C analysis to study carbonaceous aerosols. Specifically, at the Canadian Alert station, studies investigating $\delta^{13}$C changes in the EC (Rodríguez et al., 2020; Winiger et al., 2019) and springtime $\delta^{13}$C changes in the total carbon (TC) (Narukawa et al., 2008) have recently been published.

Carbonates are strongly enriched in $^{13}$C, with relatively positive $\delta^{13}$C around zero, and can thus affect $\delta^{13}$C values in the TC of TSP aerosols, as demonstrated by Chen et al. (2016) for Asian desert dust. In the Arctic region, observed higher aerosol $\delta^{13}$C values in atmospheric aerosols are often attributed to dissolved particulate organic matter from marine aerosol sources, while the influence of carbonates is ignored (Gu et al., 2023). We hypothesized that the influence of carbonates on Arctic aerosols is not negligible. In this study, we present 2 years of carbonaceous aerosol observations at Alert, focusing on carbonate content and the isotopic composition of $\delta^{13}$C of TC.

## 2 Experiments

### 2.1 Measurement site and sampling

TSP samples were collected at the WMO Global Atmosphere Watch Observatory at Alert, Nunavut, Canada (82°27′03.0″ N, 62°30′26.0″ W; 210 m a.s.l.). The Alert site represents a remote Arctic area located on the northeastern tip of Ellesmere Island, which is 817 km from the North Pole (Fig. 1). The site has been used for research on atmospheric aerosols since the mid-1980s (Barrie and Barrie, 1990). In terms of carbonaceous aerosols, BC has been measured at the station for decades (Sharma et al., 2004, 2017). Later, Rodríguez et al. (2020) reported EC and OC results from TSPs between March 2014 to June 2015, with a focus on EC analyses.

For this study, TSP samples were collected from 13 June 2016 to 16 April 2018 using a high-volume sampler on pre-baked (450 °C, 12 h) quartz fiber filters (20 × 25 cm, PALL, 2500QAT-UP). During this period, a total of 93 samples were collected at weekly intervals. The sampled filters were placed in clean glass jars with Teflon-lined caps and stored in a freezer before the chemical analyses.

### 2.2 Analyses

To obtain the TSP mass concentration, each filter was weighed before and after sampling, and resulting concentrations were corrected for the corresponding field blank filter. Subsequently, we analyzed the samples by means of two methods to measure the carbonaceous components, with the outputs shown in Fig. 2.

Contents of OC, EC, and total carbon (TC) were determined using a Sunset semi-continuous analyzer (Sunset Laboratory Inc., Tigard, OR, USA; Bauer et al., 2009) operated in offline mode. Samples with a diameter of 16 mm (area: 2.01 cm$^2$) were analyzed by means of the Improve_A temperature protocol: step [gas] temperature (°C)/duration (s) – helium (He) 140/120, He 280/120, He 480/120, He 580/120, He-$O_2$ (Ox.) 580/120, He-Ox. 740/120, He-Ox.


**Figure 1.** Map of the site position (asterisk) and geographical boundaries for dominant source regions of backward air mass trajectories (Arctic Ocean – blue, Greenland – green, northern Canada islands – red, North America – purple, Siberia – gray, and Europe – yellow). Background map by Wikimedia Commons/Public Domain.

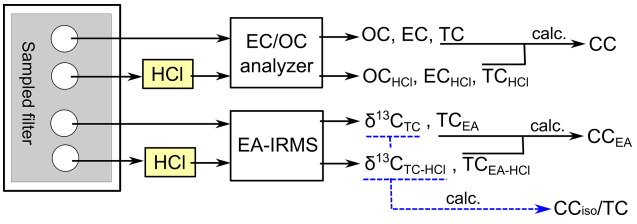


**Figure 2.** Diagram showing the method for the measurements of carbonaceous components in quartz fiber filter samples.

840/210 (Chow et al., 2007). The split point between OC and EC was determined based on laser beam (660 nm) transmittance measurements through the filter during analysis, and raw data were subsequently evaluated using RTCalc726 software (Sunset Laboratory Inc.). The same EC/OC analysis was performed after exposing the aerosol filters to HCl vapors overnight in a desiccator. From the difference between TC and $TC_{HCl}$, the content of carbonate carbon (CC) was calculated, which is discussed further in Sect. 2.3.

The same samples were further analyzed for the stable carbon isotopic composition ($\delta^{13}C$) of TC by means of the method described in more detail elsewhere (Vodička et al., 2022). Briefly, filter cuts (2.01 $cm^2$) were placed in tin cups, inserted into the elemental analyzer (EA, Flash 2000), and heated to 1000 °C in a helium atmosphere. At this temperature, carbonaceous compounds are evolved and catalytically oxidized to $CO_2$, which was isolated on a packed gas chromatograph and then measured for TC by a thermal conductivity detector and finally transferred into the isotope ratio mass spectrometer (IRMS; Delta V, Thermo Fisher Scientific) via a Conflo IV interface for the analyses of $^{13}C$ / $^{12}C$ ratios. An external standard, acetanilide (supplied by Thermo Electron Corp.), with a $\delta^{13}C$ of −27.26 ‰ compared to the Vienna Pee Dee Belemnite (VPDB), was used to obtain calibration curves for total carbon (TC) and its isotopic values. Subsequently, we determined the $\delta^{13}C$ of TC using Eq. (1) in relation to the international standard VPDB.

$$\delta^{13}C(‰) = \left[\left(^{13}C/^{12}C\right)_{sample} / \left(^{13}C/^{12}C\right)_{standard} - 1\right] \cdot 10^3 \quad (1)$$

In this manner, $\delta^{13}C_{TC}$, corresponding to delta TC values on the filter, and $\delta^{13}C_{TC-HCl}$, representing delta values on filters after exposure to HCl vapor, were analyzed. The standard deviation of $\delta^{13}C$ measurements based on triplicate sample analysis was 0.03 ‰.

Through these analyses, we obtained TC from two independent analytical techniques. We observed good agreement between the TC value measured by the EC/OC analyzer and those measured by the EA ($r = 0.98$). We also obtained a good agreement even after HCl treatment of the filters ($r = 0.98$) (Fig. S1 in the Supplement). The slightly higher TC concentrations using the EA (2 %) may be due to the use of a higher maximum temperature (1000 °C vs. 840 °C) for sample release.

### 2.3 Characteristics of carbonate carbon (CC)

Concentrations of CC, one of the key variables of this study, were calculated from the difference in TC before and after HCl fumigation (Eq. 2).

$$CC = TC - TC_{HCl} \quad (2)$$

Equation (2) defines CC or nominal CC. This procedure is probably not able to analyze all carbonates (Baudin et al., 2023), but, quantitatively, this method leads to the analysis of at least 90 % of the carbonates in samples (Karanasiou et al., 2011). Figure 3 shows thermograms from OC–EC analyses of a selected sample without HCl treatment (purple curve) and after HCl treatment (green curve). As shown in Fig. 3, the largest material loss can be seen at the temperature step EC2, but, for other samples, we observed the largest material losses in the EC1 and OC4 regions as well. These are temperature steps during which we should expect the release of carbonate carbon (CC) (Cavalli et al., 2010; Chow et al., 1993). On the other hand, removal of carboxylic acids (e.g., acetic or oxalic acid) can be expected at temperature steps OC2 and OC3 (Hasegawa, 2022). Exposing samples to HCl can also affect the transformation of organic matter, which is then released at higher temperatures. Therefore, the thermogram after fumigation may not reflect only the expected CC loss (Jankowski et al., 2008). We also analyzed several carbonate

and oxalate salt standards as a control (Fig. S2). The thermogram of the sample with a pronounced peak in the EC2 region (Fig. 3) was most similar to that of $CaCO_3$ (Fig. S2a). Hence, it can be assumed that the significant peaks, removed by HCl in the EC2 region of the thermogram, are carbonate in origin. Nevertheless, it cannot be excluded that some of the prominent CC peaks in the OC4 region are also from oxalates, as also confirmed by additional analyses of $CaCO_3$ and potassium oxalate monohydrate standards before and after HCl fumigation (Fig. S2b). The nominal CC may contain other minor carbon components. Here, however, it should also be noted that the reported values of oxalates in the Arctic (see, e.g., Feltracco et al. (2021), Svalbard) are an order of magnitude lower than the CC values we analyzed.

It is worth noting here that, if we did not analyze CC, it would be determined as either OC or EC based on the thermogram and automatic determination of the split point (Fig. 3). For both EC and OC, we calculated the percentage of mass removed by HCl fumes as CC using Eqs. (3) and (4).

$$\mathrm{EC_{removed}}\,(\%) = (\mathrm{EC} - \mathrm{EC_{HCl}})\,/\mathrm{EC} \cdot 100 \quad (3)$$

$$\mathrm{OC_{removed}}\,(\%) = (\mathrm{OC} - \mathrm{OC_{HCl}})\,/\mathrm{OC} \cdot 100 \quad (4)$$

In this way, we found that the CC contribution was, on average, 25 % (ranging from 0 % to 81 %) EC and 12 % (ranging from 0 % to 46 %) OC, which would have been inaccurately determined if we had not assessed the CC contribution. On a relative basis, EC concentrations were more biased in all seasons (Fig. S3).

Analyses for CC were performed by two independent methods (EC/OC and EA instruments, Fig. 2), and the resulting CC values show acceptable agreement (Fig. S4). Figure S4 shows that CC values based on analyses from the EC/OC analyzer may be slightly underestimated. However, unless otherwise stated, CC values calculated from EC/OC analyses are discussed in this study.

## 2.4 Estimate of $\delta^{13}$C values of CC

The $\delta^{13}$C analyses of TC and $\mathrm{TC_{HCl}}$ allowed us to estimate $\delta^{13}$C of CC. Here, we calculate the $\delta^{13}$C values of released CC on HCl fumigation using the following reaction and the isotopic mass balance equation (Eq. 5), being similar to the calculation in Kawamura and Watanabe (2004):

$\mathrm{TC} + \mathrm{HCl} \rightarrow \mathrm{CO_2}$ (carbonate carbon) $+ \mathrm{TC_{HCl}}$,

$$\delta^{13}\mathrm{C_{TC}} = f \cdot \delta^{13}\mathrm{C_{CC}} + (1-f) \cdot \delta^{13}\mathrm{C_{TC-HCl}}, \quad (5)$$

where $f$ means a fraction of CC in TC. From Eq. (5), we derived the formula for calculating $\delta^{13}\mathrm{C_{CC}}$ (Eq. 6).

$$\delta^{13}\mathrm{C_{CC}} = \left(\delta^{13}\mathrm{C_{TC}} - (1-f) \cdot \delta^{13}\mathrm{C_{TC-HCl}}\right)/f \quad (6)$$

The $\delta^{13}\mathrm{C_{CC}}$ values were reasonable for a CC content in the TC of approximately above 20 % (Fig. S5). When $f$ (CC contribution) is high, $\delta^{13}\mathrm{C_{CC}}$ values are close to zero, supporting the fact that CC is mainly composed of carbonate, such as $CaCO_3$. However, when the $f$ values are low, the $\delta^{13}\mathrm{C_{CC}}$ values are highly scattered, indicating that the carbon released (removed) by HCl is not only carbonate carbon but also contains various types of carbon including semi-volatile organic acids or unknown species. In the case of organic acids, $\delta^{13}$C values can be as high as −10 ‰ (e.g., Wang and Kawamura, 2006) or positive due to unknown isotope fractionation during analytical processing. Highly scattered values may also be due to potential analytical errors in EA-IRMS measurements when $f$ is sufficiently small. If the CC contribution were to be zero, Eq. (6) would lead to division by zero. This may also be the cause of bias and the scattering of $\delta^{13}\mathrm{C_{CC}}$ values with low CC contributions (Fig. S5).

## 2.5 Carbonate estimation from isotopic composition

We used the isotopic mass balance between $\delta^{13}\mathrm{C_{TC}}$ and $\delta^{13}\mathrm{C_{TC-HCl}}$ as an alternative and probably more accurate method to determine carbonate content ($\mathrm{CC_{iso}}$) in TC. The $\mathrm{CC_{iso}}$/TC ($f_{\mathrm{iso}}$) calculation is based on the assumption that the $\delta^{13}$C of carbonates is around 0 ‰, with an approximate range +5 ‰ to −5 ‰, and that no other compounds are present in this range. We used Eq. (5), where $\delta^{13}\mathrm{C_{TC}}$ and $\delta^{13}\mathrm{C_{TC-HCl}}$ are known, and $\delta^{13}\mathrm{C_{CC}}$ is given by three different values, covering an approximate range of carbonates (+5 ‰, 0 ‰, −5 ‰).

If

$$\delta^{13}\mathrm{C_{CC}} = 0,\ f = 1 - \left(\delta^{13}\mathrm{C_{TC}}/\delta^{13}\mathrm{C_{TC-HCl}}\right), \quad (7)$$

while

$$\delta^{13}\mathrm{C_{CC}} = +5, \text{or} -5,\ f = \left(\delta^{13}\mathrm{C_{TC}} - \delta^{13}\mathrm{C_{TC-HCl}}\right) / \left(\delta^{13}\mathrm{C_{CC}} - \delta^{13}\mathrm{C_{TC-HCl}}\right). \quad (8)$$

The $f_{\mathrm{iso}}$ value is then an average calculated from the three $f$ values obtained from Eqs. (7) and (8).

## 2.6 Auxiliary data

Air mass back trajectories (AMBTs) were calculated using the National Oceanic and Atmospheric Administration (NOAA) HYSPLIT model (Stein et al., 2015) at 500 m a.g.l. using a run time of 168 h in GDAS (Global Data Assimilation System) with 0.5° resolution for each sampling day. For subsequent analyses, we divided the air masses into six sectors, as depicted in Fig. 1.

Meteorological data at 5 min resolution for temperature ($T$), wind speed (WS), and wind direction (WD) were provided by Environment and Climate Change Canada. Only WDs between 14 November 2016 and 16 January 2017 were obtained from the NOAA website (https://psl.noaa.gov/arctic/observatories/alert/, last access: 12 June 2024). For the

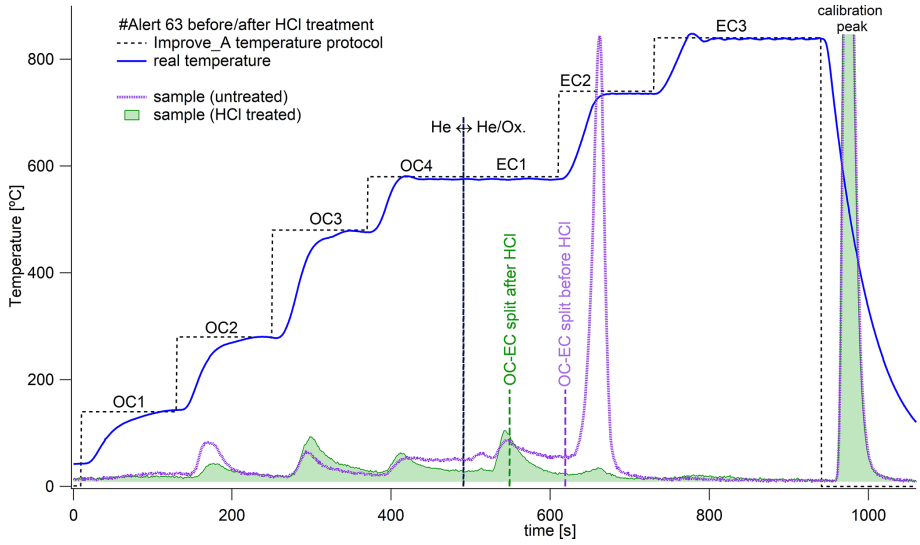


**Figure 3.** Example of EC/OC analysis of untreated (purple thermogram) and treated sample with HCl fumigation (green thermogram) by means of Improve_A temperature protocol. The vertical dashed black line shows a change in the use of He and the He-Ox mixture in the analysis. The vertical dashed green and purple lines show the automatic determination of the split point between OC and EC. Sample no. Alert-63 was collected from 15 to 22 May 2017.

purpose of this study, complementary mean values of $T$ and WS were calculated in relation to each sample.

The WD and WS data were used to create wind roses using Zefir software (Petit et al., 2017) and were used in combination with the AMBT data to determine the predominant aerosol origin for each sample. All wind roses and AMBTs by HYSPLIT are shown in the supplementary data.

The water-soluble ions ($Ca^{2+}$, $Mg^{2+}$, $Na^{+}$) were measured using ion chromatography (761 Compact IC, Metrohm, Switzerland). For this purpose, the filtered samples were extracted twice with 10 mL of ultrapure water using an ultrasonic bath for 15 min, and the aqueous extracts were filtered using a disc filter (Millex-GV, 0.22 µm, Millipore).

## 3 Results and discussion

### 3.1 Carbonaceous aerosol composition

Time series of TC, $OC_{HCl}$, $EC_{HCl}$, and CC mass concentrations are shown in Fig. 4. An overview of results is provided for the seasonal variations from 2016 to 2018 in Table 1 and Fig. S6. An average TC concentration over the entire measurement period was $0.219 \pm 0.147\,\mu g\,m^{-3}$ (median of $0.186\,\mu g\,m^{-3}$; deviation due to one sample with a concentration of $1.22\,\mu g\,m^{-3}$, Fig. 4a). The average TC contribution in the aerosol mass ranged from 5 % to 14 % (Table 1). Seasonally, the highest mass concentrations of TC, $OC_{HCl}$, and $EC_{HCl}$ were found in winter and/or spring (Fig. S6, Table 1).

The fact that $EC_{HCl}$ corresponds to realistic elemental carbon concentrations is demonstrated by comparison with the study of Rodríguez et al. (2020), in which EC in TSPs was analyzed during 2014–2015. They reported seasonal EC concentrations that are similar to our observed $EC_{HCl}$, while their CC was part of the OC due to the use of a different temperature protocol (EnCan-Total-900) during the OC/EC analysis. However, Rodríguez et al. (2020) did not quantify the contribution of CC to TC.

Concentrations of $OC_{HCl}$ dominate in all seasons (Figs. 4b and 5) but present seasonally different correlations with ambient temperature. Especially in summer, we observe a significant positive correlation ($r = 0.73$) between $OC_{HCl}$ concentrations and temperature (Fig. S7a). A similar relationship was also observed, e.g., at the subarctic station Pallas (Friman et al., 2023), suggesting a biogenic origin of summertime organic aerosols in Arctic areas (Moschos et al., 2022). In contrast, we observe negative correlations between $OC_{HCl}$ and ambient temperature in winter ($r = -0.15$, insignificant) and spring ($r = -0.43$). A year-round similar trend was observed for $EC_{HCl}$ ($r = -0.39$, Fig. S7b), supporting previous studies that highlight, in particular, the anthropogenic contributions to Arctic aerosol during the polar night (Moschos et al., 2022). However, for CC, we observe no significant dependence on temperature ($r = 0.09$, Fig. S7c).

Time series of TC before and after HCl fumigation (Fig. 4a) show that the amount of carbon removed in the form of CC is neither negligible nor large. However, both mass concentrations of CC (Fig. 4b) and its relative contributions (Fig. 4c) show that the CC is often larger than the $EC_{HCl}$ contribution. Specifically, CC concentrations were highest during both the autumn of 2016 and the summer of 2016 and 2017 (Fig. S6c), which were also reflected in the relative contributions to TC (Table 1, Fig. 5).

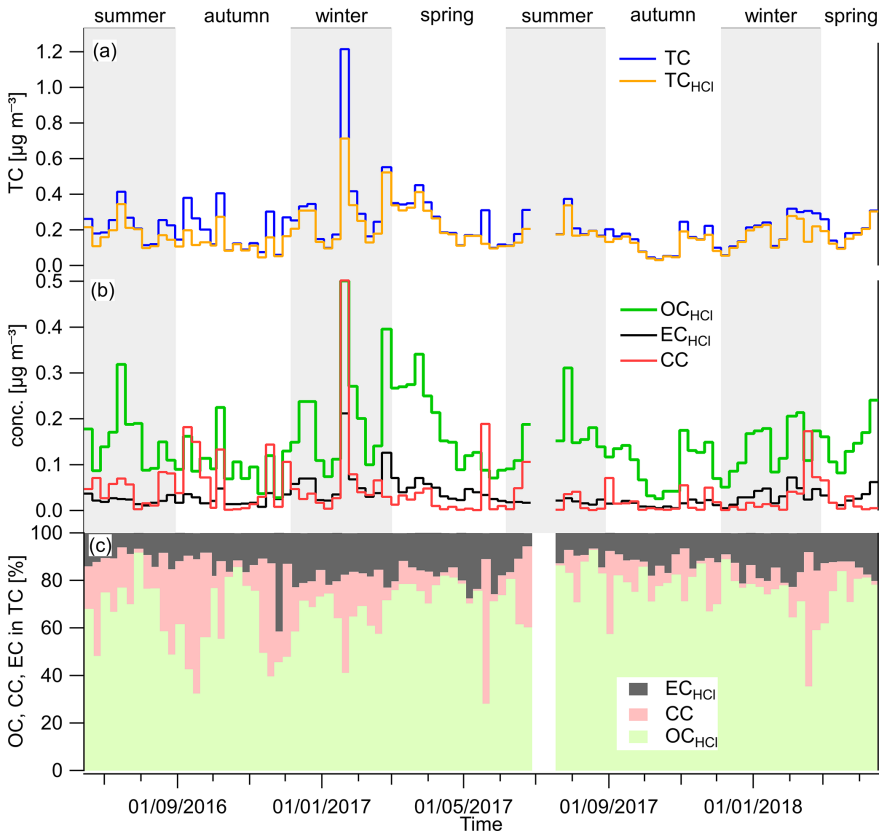


**Figure 4.** Time series of **(a)** TC mass concentrations before and after HCl treatment of samples; **(b)** OC, EC, and CC mass concentrations; and **(c)** their relative contributions to TC in the Alert TSP aerosols.

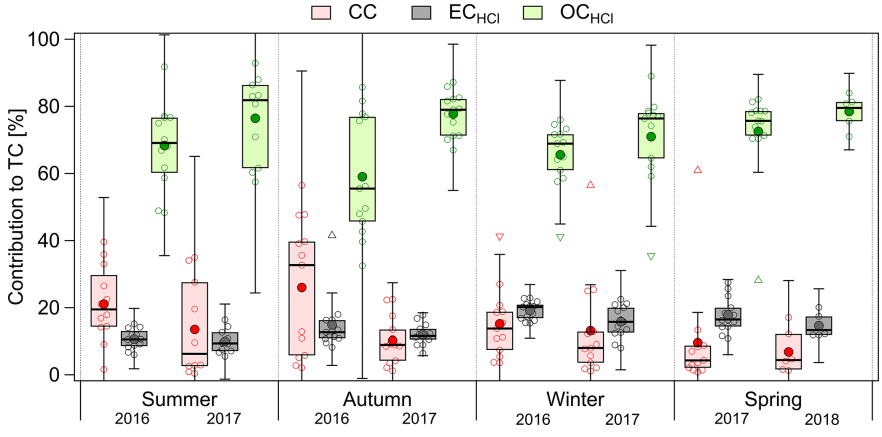


**Figure 5.** Seasonal contributions of CC, $EC_{HCl}$, and $OC_{HCl}$ to TC. The boxes correspond to the interquartile range (IQR; 25th and 75th percentile), with the median represented by the inner solid line. The whiskers correspond to the inner fence range ($1.5 \cdot IQR$), triangles are outliers, and the mean is represented by the large filled circle.

It is worthwhile to understand the origin of CC. During summer, the contribution of biogenic aerosols (a potential source of oxalates) is highest, while the landscape is least covered by snow, making the situation favorable for resuspension of soils eroded from rocks, including carbonates. A potential source of carbonates may come directly from the Canadian Arctic land region, where limestone sediments are reported to be abundantly present (Groot Zwaaftink et al., 2016; Not and Hillaire-Marcel, 2012; Phillips and Grantz, 2001). Another likely source of carbonate is marine aerosols as marine organisms contribute carbonate to the sea (Stein et

**Table 1.** Seasonal averages ± standard deviations (medians in parentheses) of different variables in TSPs at Alert site.

| | Summer 2016 | Autumn 2016 | Winter 2016 | Spring 2017 | Summer 2017 | Autumn 2017 | Winter 2017 | Spring 2018 |
|---|---|---|---|---|---|---|---|---|
| N | 12 | 13 | 13 | 13 | 10 | 13 | 13 | 6 |
| OC | 0.182 ± 0.075 | 0.136 ± 0.072 | 0.253 ± 0.171 | 0.184 ± 0.092 | 0.179 ± 0.071 | 0.106 ± 0.06 | 0.154 ± 0.057 | 0.154 ± 0.053 |
| [μg m$^{-3}$] | (0.177) | (0.106) | (0.237) | (0.151) | (0.155) | (0.128) | (0.177) | (0.153) |
| EC | 0.037 ± 0.021 | 0.056 ± 0.055 | 0.100 ± 0.121 | 0.057 ± 0.037 | 0.031 ± 0.015 | 0.019 ± 0.013 | 0.055 ± 0.036 | 0.032 ± 0.018 |
| [μg m$^{-3}$] | (0.032) | (0.023) | (0.070) | (0.047) | (0.026) | (0.017) | (0.046) | (0.029) |
| TC | 0.219 ± 0.082 | 0.193 ± 0.120 | 0.353 ± 0.287 | 0.240 ± 0.113 | 0.210 ± 0.076 | 0.125 ± 0.070 | 0.209 ± 0.088 | 0.186 ± 0.071 |
| [μg m$^{-3}$] | (0.216) | (0.126) | (0.290) | (0.186) | (0.186) | (0.146) | (0.225) | (0.182) |
| $OC_{HCl}$ | 0.150 ± 0.067 | 0.103 ± 0.052 | 0.215 ± 0.125 | 0.172 ± 0.088 | 0.159 ± 0.062 | 0.096 ± 0.051 | 0.140 ± 0.052 | 0.146 ± 0.056 |
| [μg m$^{-3}$] | (0.144) | (0.095) | (0.201) | (0.149) | (0.150) | (0.111) | (0.161) | (0.138) |
| $EC_{HCl}$ | 0.022 ± 0.008 | 0.024 ± 0.012 | 0.067 ± 0.052 | 0.040 ± 0.015 | 0.019 ± 0.004 | 0.014 ± 0.007 | 0.034 ± 0.018 | 0.029 ± 0.018 |
| [μg m$^{-3}$] | (0.022) | (0.021) | (0.058) | (0.040) | (0.019) | (0.015) | (0.031) | (0.024) |
| $TC_{HCl}$ | 0.172 ± 0.070 | 0.127 ± 0.061 | 0.282 ± 0.175 | 0.211 ± 0.101 | 0.178 ± 0.064 | 0.110 ± 0.057 | 0.174 ± 0.068 | 0.175 ± 0.074 |
| [$\mu$g m$^{-3}$] | (0.165) | (0.115) | (0.250) | (0.175) | (0.169) | (0.128) | (0.194) | (0.162) |
| CC | 0.047 ± 0.028 | 0.066 ± 0.068 | 0.071 ± 0.131 | 0.029 ± 0.051 | 0.032 ± 0.036 | 0.015 ± 0.018 | 0.035 ± 0.048 | 0.011 ± 0.011 |
| [μg m$^{-3}$] | (0.052) | (0.030) | (0.034) | (0.010) | (0.020) | (0.006) | (0.014) | (0.007) |
| TC/mass | 10.3 ± 3.8 | 6.0 ± 1.9 | 7.8 ± 3.5 | 5.9 ± 2.4 | 13.2 ± 5.4 | 8.3 ± 6.2 | 6.0 ± 1.6 | 7.8 ± 1.8 |
| [%] | (9.4) | (5.9) | (8.3) | (5.4) | (13.7) | (7.3) | (5.2) | (7.3) |
| CC/TC | 21.1 ± 11.2 | 26.1 ± 19.8 | 15.2 ± 10.6 | 9.6 ± 15.9 | 13.5 ± 14.2 | 10.2 ± 7.1 | 13.2 ± 15.2 | 6.8 ± 6.4 |
| [%] | (19.5) | (32.7) | (13.8) | (4.3) | (6.2) | (8.9) | (8.0) | (4.4) |
| $CC_{iso}$/TC | 15.0 ± 9.6 | 22.0 ± 16.0 | 8.5 ± 8.5 | 7.8 ± 17.9 | 14.2 ± 12.6 | 4.6 ± 5.3 | 10.3 ± 17.4 | 1.2 ± 2.4 |
| [%] | (14.9) | (15.6) | (6.7) | (1.2) | (9.8) | (4.4) | (0.2) | (0.0) |
| $OC_{HCl}$/TC | 68.3 ± 12.5 | 59.0 ± 18.1 | 65.6 ± 9.5 | 72.5 ± 13.9 | 76.5 ± 12.8 | 77.7 ± 6.3 | 71.0 ± 13.4 | 78.5 ± 4.6 |
| [%] | (69.1) | (55.5) | (68.9) | (75.7) | (81.8) | (79.0) | (76.4) | (79.5) |
| $EC_{HCl}$/TC | 10.6 ± 3.0 | 14.9 ± 8.5 | 19.2 ± 2.7 | 17.9 ± 5.1 | 10.0 ± 3.6 | 12.0 ± 3.2 | 15.8 ± 4.7 | 14.7 ± 3.4 |
| [%] | (10.5) | (12.7) | (20.2) | (16.5) | (9.3) | (11.6) | (15.8) | (13.3) |
| $TC_{EA}$ | 0.218 ± 0.101 | 0.184 ± 0.118 | 0.345 ± 0.263 | 0.234 ± 0.119 | 0.199 ± 0.079 | 0.126 ± 0.067 | 0.227 ± 0.100 | 0.195 ± 0.083 |
| [μg m$^{-3}$] | (0.214) | (0.120) | (0.287) | (0.200) | (0.174) | (0.124) | (0.224) | (0.191) |
| $\delta^{13}C_{TC}$ | −22.7 ± 2.7 | −21.2 ± 4.5 | −24.8 ± 2.4 | −22.8 ± 4.4 | −22.6 ± 3.2 | −24.2 ± 1.6 | −23.4 ± 4.3 | −24.5 ± 0.6 |
| [‰] | (−23.0) | (−23.4) | (−25.9) | (−24.0) | (−24.0) | (−24.9) | (−25.6) | (−24.3) |
| $TC_{EA-HCl}$ | 0.141 ± 0.063 | 0.092 ± 0.052 | 0.273 ± 0.196 | 0.199 ± 0.108 | 0.157 ± 0.065 | 0.103 ± 0.052 | 0.173 ± 0.068 | 0.184 ± 0.080 |
| [μg m$^{-3}$] | (0.136) | (0.079) | (0.253) | (0.169) | (0.144) | (0.099) | (0.188) | (0.166) |
| $\delta^{13}C_{TC-HCl}$ | −26.6 ± 0.7 | −27.0 ± 1.1 | −27.1 ± 0.9 | −24.4 ± 1.1 | −26.2 ± 0.5 | −25.3 ± 0.8 | −26.0 ± 0.4 | −24.7 ± 0.8 |
| [‰] | (−26.6) | (−27.2) | (−27.0) | (−24.3) | (−26.2) | (−25.2) | (−26.1) | (−24.7) |
| WS | 5.1 ± 1.8 | 5.5 ± 2.7 | 3.9 ± 2.7 | 3.0 ± 1.4 | 4.2 ± 1.8 | 2.5 ± 1.2 | 3.6 ± 1.8 | 2.7 ± 0.6 |
| [m s$^{-1}$] | (4.5) | (5.6) | (3.1) | (3.5) | (4.6) | (2.1) | (3.4) | (2.6) |
| Temp. | 5.0 ± 4.6 | −13.8 ± 6.9 | −28.7 ± 4.0 | −20.5 ± 8.4 | 1.2 ± 4.6 | −18.6 ± 6.8 | −26.2 ± 3.9 | −30.0 ± 3.5 |
| [°C] | (4.2) | (−14.0) | (−27.6) | (−21.3) | (1.5) | (−19.6) | (−25.5) | (−30.8) |

al., 1994). In the context of wind directions and the effect on $\delta^{13}C$, the origin of CC is further discussed in Sect. 3.2.

### 3.2 Stable carbon isotopic composition

Removal of CC by HCl fumigation has a significant effect on the measurements of the $\delta^{13}C$ isotopic values of TC (Figs. 6 and 7). Figure 6 shows seasonally resolved $\delta^{13}C$ values for HCl-treated (red) and untreated (gray) samples. We observed significant changes in all seasons, except for the spring of 2017 and 2018. Here, it is interesting to mention a link with Narukawa et al. (2008), who reported changes in the $\delta^{13}C$ of TC values for HCl-treated samples between winter and spring at the Alert site. Narukawa et al. (2008) show significantly higher $\delta^{13}C$ values in spring than in winter and related this to the possible contribution of carboxylic acids (especially oxalic acid). During our observations, the differences in the average values of the $\delta^{13}C$ of TC (HCl treated vs. untreated) were also significant (see red boxes in Fig. 6 and Table 1). Winter and spring $\delta^{13}C$ values after HCl treatment in this study (Table 1) are similar to those presented by Narukawa et al. (2008) for the year 2000. Thus, this study confirms that this is a long-term phenomenon that is likely to occur annually.

In addition, measurements of $\delta^{13}C$ in OC, pyrolytic carbon (POC)–CC, and EC, performed at Environment Canada Toronto Laboratory using the ECT9 temperature protocol (Huang et al., 2006, 2021) for the fine-particle ($PM_1$) samples collected around 2003, support the fact that a noticeable fraction of CC occurs during the summer months, as indicated by the relatively more positive $\delta^{13}C$ of the POC–CC fraction (Fig. S8). Carbonate from eroded rocks in terrestrial environments usually generates large particles, and so the CC content in $PM_1$ should be lower than that in TSPs. Consequently, the $\delta^{13}C$ TC in $PM_1$ is expected to be rel-

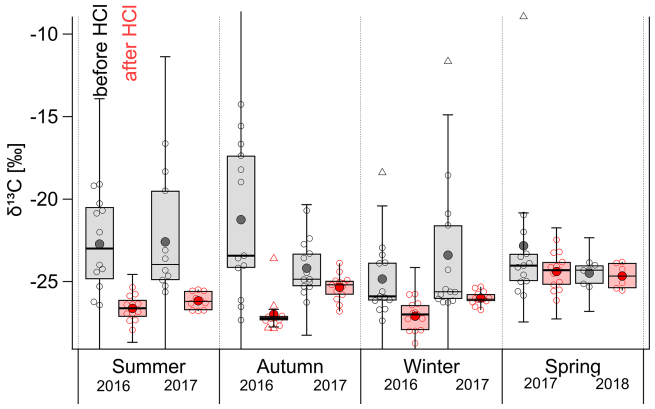


**Figure 6.** Seasonal variations in the $\delta^{13}C$ of TC of untreated (gray) and HCl-treated (red) TSP samples at the Alert site from summer 2016 to spring 2018. The boxes correspond to the interquartile range (IQR; 25th and 75th percentile), with the median represented by the inner solid line. The whiskers correspond to the inner fence range ($1.5 \cdot$ IQR), triangles are outliers, and the mean is represented by the large filled circle.

atively less positive compared to that in TSPs. Therefore, Fig. S8 suggests that the impact of CC on $\delta^{13}C$ TC is an annual phenomenon occurring over decadal periods. The tendency towards relatively more positive $\delta^{13}C$ in summer OC fractions also suggests the presence of minor salt oxalates or potassium or magnesium carbonates, which are released at 550 °C or lower, as shown in Fig. S2. In the time series in Fig. 7, we observed episodes with significant differences in $\delta^{13}C$ values, alternating over short periods. The comparison of the $\delta^{13}C$ of TC and TC mass concentrations for both HCl-untreated and treated samples shows insignificant correlation (Fig. S9). However, we found a significant, though not strong, correlation of $\delta^{13}C$ with wind speed (Fig. S10) ($r = 0.36$) and a negative correlation after HCl fumigation ($r = -0.32$ for $\delta^{13}C_{TC-HCl}$ vs. wind speed). Concentrations of CC were also positively correlated with wind speed ($r = 0.48$, Fig. S10), indicating that wind has an effect on this aerosol component. Therefore, we compared the $\delta^{13}C$ time series with average wind speeds and prevailing AMBTs from the HYSPLIT model (see colored bars in Fig. 7), which were divided into six regions, as shown in Fig. 1.

The large differences in $\delta^{13}C$ values (or relatively more positive $\delta^{13}C_{TC}$ values) can be divided into three categories. The most frequent differences were observed during periods of stronger winds (average WS above $4\,m\,s^{-1}$) associated with the prevailing back trajectories from the northern Canada region. These episodes can be found mainly in the summer and autumn of 2016 and the summer of 2017. Such conditions favor dust resuspension, which may also contain limestone, known to be abundant in this region (Not and Hillaire-Marcel, 2012; Phillips and Grantz, 2001). The presence of a peak in soil dust carbonates in late summer/early autumn is consistent with multidecadal aerosol aluminum observations at Alert (Sharma et al., 2019; Sirois and Barrie, 1999). These observations also indicate a peak in soil dust aerosol in the spring month of May (Sharma et al., 2019).

Second, in late February–March 2018, we observed significant enrichment of $^{13}C$, which may be linked to long-range transport (LRT) from and/or over Europe, Greenland, and North America (Fig. 6). Sources of carbonate, in this case, may be, for example, calcifying marine phytoplankton (Monteiro et al., 2016), abundant in the North Atlantic (Okada and Honjo, 1973). Another possibility is the volcanic and subarctic semi-desert areas in Iceland (Arnalds et al., 2016).

The third case is a $\delta^{13}C$ difference observed during lower wind speeds coming from the Arctic Ocean or Greenland. This also includes the sample taken between 15–22 May 2017, whose thermograms are shown in Fig. 3 and which was most enriched in $^{13}C$ carbon. A recent study by Gu et al. (2023), which reports observations of summer carbonaceous aerosols in the Arctic Ocean, is relevant in this context. The aforementioned authors also observed relatively more negative $\delta^{13}C$ values of TC, but, in this case, they did not consider the enriched $^{13}C$ carbon as a carbonate contribution; instead, they associated it with an input of fresh marine particulate organic carbon (MPOC) (Verwega et al., 2021). MPOC is formed by the conversion of inorganic carbon by marine phytoplankton through photosynthesis in the ocean surface layer (Descolas-Gros and Fontugne, 1990), and this carbon can be partially released into the atmosphere as marine aerosol (Ceburnis et al., 2016). We cannot exclude the influence of MPOC on the TSPs taken at the Alert station, but, instead, the specific EC/OC thermogram (Figs. 3, S2) shows an influence of $CaCO_3$. The presence of carbonates in surface seawater and their interference with organic coatings have been known about for decades (Chave, 1965). Dissolved $CO_2$ in the oceans consists mainly of inorganic substances, which are bicarbonates ($HCO_3^-$; > 85 %) and carbonates (ca. 10 %), and their content varies with temperature, pH, salinity, and other parameters (Zeebe, 2012). Carbonate, in the form of $CaCO_3$, is generally supersaturated in surface seawater, but its precipitation may be limited due to dissolved organic matter (Chave and Suess, 1970). In addition to common inorganic reactions due to dissolved $CO_2$, the carbonate cycle is also influenced by marine life. Phytoplankton such as coccolithophores (e.g., *Emiliania huxleyi*) could also contribute to the formation of carbonates (Smith et al., 2012). These organisms produce calcified shells called coccoliths, which are about 2–25 µm across (Monteiro et al., 2016). While these microfossils are mostly deposited on the seabed, they are also likely to be released into the atmosphere with marine aerosol from the upper sea layers. Such a potential introduction of coccolith fragments by sea spray aerosol into the atmosphere is reported by Mukherjee et al. (2020) for the Arctic summer. Whether through MPOC or inorganic carbon, this phytoplankton influences the fractionation of $^{13}C$ carbon (Holtz et al., 2017).

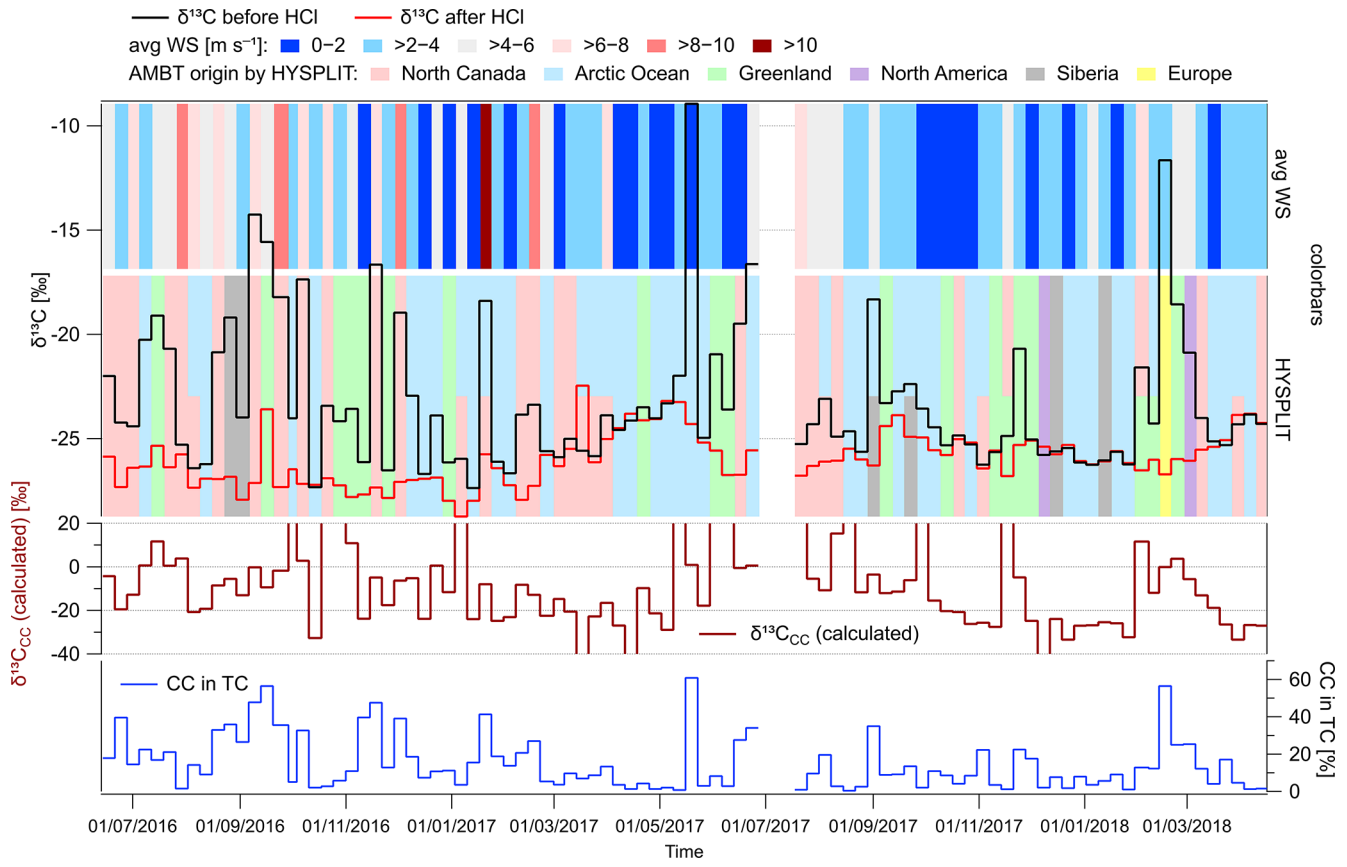


**Figure 7.** Time series of isotopic composition ($\delta^{13}C$) of TC before and after HCl treatment of samples (upper part), with color bars representing average wind speed (top) and origin of AMBTs based on HYSPLIT model and divided to regions as shown in Fig. 1 (middle part). Time series of the calculated $\delta^{13}C_{CC}$ (outliers less than −40 ‰ and more than +20 ‰ not depicted) and contribution of CC in TC (bottom).

Coccolith microfossils contain enriched calcite with $\delta^{13}C$ values around 0 ‰ (McClelland et al., 2017). Limestone sediments in the Canadian Arctic are even more enriched, with $\delta^{13}C$ values ranging from 2 ‰ to 8 ‰ (Beauchamp et al., 1987). After estimating $\delta^{13}C_{CC}$ (see Sect. 2.4), we observed that, with a high CC abundance in TC, the calculated $\delta^{13}C_{CC}$ values are also seen around 0 ‰ (Figs. 7 (bottom), S5). This suggests that, when the TC contains a larger contribution of CC (suppose above 20 %), it can be assumed that a significant portion of the nominal CC is derived from limestone. However, the uncertainties in the determination of $\delta^{13}C_{CC}$, mentioned in Sect. 2.4, primarily due to the low CC contributions in TC, likely prevent the distinction of whether the carbonates are from sediment resuspension or marine calcified shells. Some insight, however, can be obtained from the AMBT analysis discussed earlier.

Finally, Fig. 8a confirms a strong dependence of $\delta^{13}C_{TC}$ on the CC content in TC ($r = 0.79$). The direct dependence of $\delta^{13}C_{TC}$ on CC mass concentration is even stronger ($r = 0.85$ after excluding one outlier, Fig. S11). Furthermore, we calculated the fractions of CC for individual samples via isotope mass balance (using $\delta^{13}C$ with a CC value of zero as the endmember; see Sect. 2.5.) and found that, overall, the calculated results were approximately 5 % lower than the measured CC/TC, with less scatter. In addition, we observed an excellent correlation between the $\delta^{13}C$ of TC and the calculated fraction of CC, with $r = 0.96$, as shown in Fig. 8b, indicating that more than 92 % of the variation in the $\delta^{13}C$ of TC can be explained by the dependency on the fraction of CC.

Further support for the influence of the $\delta^{13}C$ of TC in favor of carbonates is provided by its strong correlation with calcium ($r = 0.89$, Fig. 8c). Calcium is also strongly correlated with CC contributions in TC, with $r = 0.90$ for Ca vs. $CC_{iso}$/TC (Fig. 8d). Apportionment of Ca amongst aerosol sources at the Alert site (Sharma et al., 2019), using multi-decadal observations and positive matrix factorization analyses, showed that, on average, for the periods of both November to February and March to May, Ca was associated (84 % and 85 %, respectively) with windblown dust or soil and (12 % and 8 %, respectively) with sea salt aerosol.

We also investigated the possible contribution of carbon from magnesium carbonate. Magnesium was strongly correlated with sodium ($r = 0.91$, Fig. S12), indicating its primary

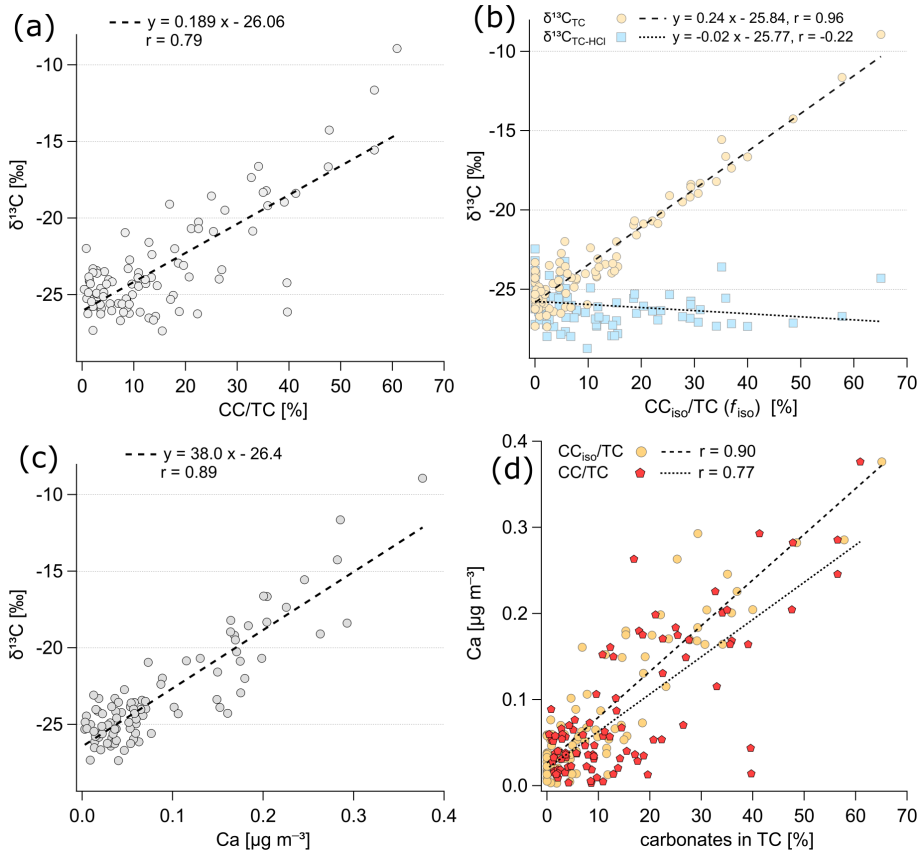


**Figure 8.** Dependence of **(a)** $\delta^{13}C_{TC}$ on the percentage contribution of CC in TC, **(b)** $\delta^{13}C_{TC}$ and $\delta^{13}C_{TC-HCl}$ on the calculated fraction of $CC_{iso}$ in TC, **(c)** $\delta^{13}C_{TC}$ on Ca mass concentrations, and **(d)** Ca mass concentrations on percentage contribution of CC and $CC_{iso}$ in TC.

link to marine aerosol. In contrast, we observed no relationship between Mg and Ca; this dependence was strongly scattered (Fig. S12). Overall, the results indicate that the main contribution of CC, which strongly influences the $\delta^{13}C$ of TC, is mainly $CaCO_3$. If there is a contribution of magnesium carbonate, it is rather episodic.

These results thus provide evidence that the CC content in aerosols, mostly of soil origin and, to a lesser extent, marine origin, strongly influences the $\delta^{13}C$ isotopic composition of TC in the Arctic atmosphere. Further research at different Arctic sites could reveal whether the non-negligible presence of CC in the TSP is the case only in the northern Canada region or a phenomenon observed in larger parts of the Arctic.

## 4 Summary and conclusions

We found that the aerosol CC (i.e., carbonate carbon) fraction in Arctic TSPs at the Alert site is not negligible. The relative abundances of CC in TC ranged from 0 % to 60 %, with an average of 11 % over the entire measurement period. On average, 25 % (range: 0 % to 81 %) of EC and 12% (range: 0 to 46 %) of OC was identified here as nominal CC. The influence of CC removal from the sample was also significantly reflected in the isotopic composition of the $\delta^{13}C$ of TC. The effect of CC on $\delta^{13}C$ was particularly pronounced in the summer of 2016 and 2017, as well as during the autumn of 2016 due to strong local Arctic dust transport. In contrast, the effect of removing of CC on $\delta^{13}C$ was lowest in spring. Thus, CC content in TSPs at Alert can sometimes strongly influence the $\delta^{13}C$ values of aerosols.

Based on the thermograms from EC/OC analyses and the calculated $\delta^{13}C_{CC}$, whose values were around 0 ‰ at high CC contributions to TC, we conclude that the major part of CC is derived from carbonates. Additionally, based on the isotope mass balance calculation (using 0 ‰ as $\delta^{13}C_{CC}$), an excellent dependency between the $\delta^{13}C$ of TC and the calculated fraction of CC ($r = 0.96$) is observed, supporting the fact that most of the variations in the $\delta^{13}C$ of TC were due to the contribution of CC. Based on the AMBT analyses, we identified two possible carbonate sources. The first is eroded and resuspended limestone sediments in the northern Canadian region. The second source may be calcareous shells (coccoliths) produced by marine phytoplankton and transported from both the Arctic Ocean and the North Atlantic Ocean. However, the hypothesis of these sources requires further detailed research.

In general, when analyzing the $\delta^{13}C$ of TC in coarse aerosol or aerosols laden with dust, it must be taken into account that the resulting values may be strongly influenced by CC content. If CC is not removed prior to EC/OC analysis, CC may be mistakenly identified as EC during Improve_A analysis. This could, for example, affect modeling of the effect of carbonaceous aerosols on the Arctic climate as EC (or black carbon) has a warming effect on the atmosphere, while CC has a lower warming effect.

**Data availability.** All relevant data for this paper are archived and are available upon request from the corresponding authors or online at the following repository: https://doi.org/10.5281/zenodo.16994150 (Vodička, 2025).

**Supplement.** The supplement related to this article is available online at https://doi.org/10.5194/acp-25-10215-2025-supplement.

**Author contributions.** All of the authors contributed to the final version of this article. PV analyzed EC/OC before and after HCl treatment, as well as the $\delta^{13}C$ of TC; conducted the AMBT analyses; evaluated all of the data; and wrote the paper under the supervision of KK. BK analyzed the $\delta^{13}C$ of TC after HCl treatment and supported the water-soluble-ion measurements. LH calculated the contribution of $CC_{iso}$/TC based on $\delta^{13}C$ measurements. DK and MMH assisted in the gravimetry and other sample treatments. AP was responsible for the evaluation of Ca, Mg, and Na data. SS provided meteorological data. SS, with KK and LB, managed the field campaign. All of the authors provided advice and feedback throughout the drafting and submission process.

**Competing interests.** At least one of the (co-)authors is a member of the editorial board of *Atmospheric Chemistry and Physics*. The peer-review process was guided by an independent editor, and the authors also have no other competing interests to declare.

**Disclaimer.** Publisher's note: Copernicus Publications remains neutral with regard to jurisdictional claims made in the text, published maps, institutional affiliations, or any other geographical representation in this paper. While Copernicus Publications makes every effort to include appropriate place names, the final responsibility lies with the authors.

**Acknowledgements.** This study was supported by JSPS grant no. 24221001; the JSPS Joint Research Program implemented in association with DFG (JRPs-LEAD with DFG, grant no. JPJSJRP 20181601); and the Ministry of Education, Youth and Sports of the Czech Republic under project no. ACTRIS-CZ LM2023030. The authors thank the CFS Alert for maintaining the base, as well as Andrew Platt (Alert coordinator), the operator for ECCC, and the students for the sample collection at Alert and the shipment of these samples.

**Financial support.** This research has been supported by the Japan Society for the Promotion of Science (grant nos. 24221001 and JPJSJRP 20181601) and the Ministerstvo Školství, Mládeže a Tělovýchovy (grant no. ACTRIS-CZ LM2023030).

**Review statement.** This paper was edited by Yugo Kanaya and reviewed by two anonymous referees.

## References

Arnalds, O., Dagsson-Waldhauserova, P., and Olafsson, H.: The Icelandic volcanic aeolian environment: Processes and impacts – A review, Aeolian Res., 20, 176–195, https://doi.org/10.1016/j.aeolia.2016.01.004, 2016.

Barrie, L. A. and Barrie, M. J.: Chemical components of lower tropospheric aerosols in the high Arctic: Six years of observations, J. Atmos. Chem., 11, 211–226, https://doi.org/10.1007/BF00118349, 1990.

Baudin, F., Bouton, N., Wattripont, A., and Carrier, X.: Carbonates thermal decomposition kinetics and their implications in using Rock-Eval® analysis for carbonates identification and quantification, Sci. Technol. Energy Transit., 78, https://doi.org/10.2516/stet/2023038, 2023.

Bauer, J. J., Yu, X.-Y., Cary, R., Laulainen, N., and Berkowitz, C.: Characterization of the sunset semi-continuous carbon aerosol analyzer, J. Air Waste Ma., 59, 826–833, https://doi.org/10.3155/1047-3289.59.7.826, 2009.

Beauchamp, B., Oldershaw, A. E., and Krouse, H. R.: Upper carboniferous to upper permian $^{13}C$-enriched primary carbonates in the sverdrup basin, Canadian arctic: Comparisons to coeval Western North American Ocean Margins, Chem. Geol. Isot. Geosci. Sect., 65, 391–413, https://doi.org/10.1016/0168-9622(87)90016-9, 1987.

Carslaw, K. S., Lee, L. A., Reddington, C. L., Pringle, K. J., Rap, A., Forster, P. M., Mann, G. W., Spracklen, D. V., Woodhouse, M. T., Regayre, L. A., and Pierce, J. R.: Large contribution of natural aerosols to uncertainty in indirect forcing, Nature, 503, 67–71, https://doi.org/10.1038/nature12674, 2013.

Cavalli, F., Viana, M., Yttri, K. E., Genberg, J., and Putaud, J.-P.: Toward a standardised thermal-optical protocol for measuring atmospheric organic and elemental carbon: the EUSAAR protocol, Atmos. Meas. Tech., 3, 79–89, https://doi.org/10.5194/amt-3-79-2010, 2010.

Ceburnis, D., Masalaite, A., Ovadnevaite, J., Garbaras, A., Remeikis, V., Maenhaut, W., Claeys, M., Sciare, J., Baisnée, D., and O'Dowd, C. D.: Stable isotopes measurements reveal dual carbon pools contributing to organic matter enrichment in marine aerosol, Sci. Rep., 6, 1–6, https://doi.org/10.1038/srep36675, 2016.

Chave, K. E.: Carbonates: Association with organic matter in surface seawater, Science, 148, 1723–1724, https://doi.org/10.1126/science.148.3678.1723, 1965.

Chave, K. E. and Suess, E.: Calcium Carbonate Saturation in Seawater: Effects of Dissolved Organic Matter, Limnol. Oceanogr., 15, 633–637, https://doi.org/10.4319/lo.1970.15.4.0633, 1970.

Chen, B., Cui, X., and Wang, Y.: Regional prediction of carbon isotopes in soil carbonates for Asian dust source tracer, Atmos. Env-

iron., 142, 1–8, https://doi.org/10.1016/j.atmosenv.2016.07.029, 2016.

Chen, P., Kang, S., Abdullaev, S. F., Safarov, M. S., Huang, J., Hu, Z., Tripathee, L., and Li, C.: Significant influence of carbonates on determining organic carbon and black carbon: A case study in Tajikistan, central Asia, Environ. Sci. Technol., 55, 2839–2846, https://doi.org/10.1021/acs.est.0c05876, 2021.

Chow, J. C., Watson, J. G., Pritchett, L. C., Pierson, W. R., Frazier, C. A., and Purcell, R. G.: The dri thermal/optical reflectance carbon analysis system: description, evaluation and applications in U.S. Air quality studies, Atmos. Environ., 27, 1185–1201, 1993.

Chow, J. C., Watson, J. G., Chen, L.-W. A., Chang, M. C. O., Robinson, N. F., Trimble, D., and Kohl, S.: The IMPROVE_A temperature protocol for thermal/optical carbon analysis: maintaining consistency with a long-term database, J. Air Waste Ma., 57, 1014–1023, https://doi.org/10.3155/1047-3289.57.9.1014, 2007.

Descolas-Gros, C. and Fontugne, M.: Stable carbon isotope fractionation by marine phytoplankton during photosynthesis, Plant. Cell Environ., 13, 207–218, https://doi.org/10.1111/j.1365-3040.1990.tb01305.x, 1990.

England, M. R., Eisenman, I., Lutsko, N. J., and Wagner, T. J. W.: The Recent Emergence of Arctic Amplification, Geophys. Res. Lett., 48, https://doi.org/10.1029/2021GL094086, 2021.

Feltracco, M., Barbaro, E., Spolaor, A., Vecchiato, M., Callegaro, A., Burgay, F., Vardè, M., Maffezzoli, N., Dallo, F., Scoto, F., Zangrando, R., Barbante, C., and Gambaro, A.: Year-round measurements of size-segregated low molecular weight organic acids in Arctic aerosol, Sci. Total Environ., 763, 142954, https://doi.org/10.1016/j.scitotenv.2020.142954, 2021.

Flanner, M. G., Zender, C. S., Randerson, J. T., and Rasch, P. J.: Present-day climate forcing and response from black carbon in snow, J. Geophys. Res., 112, D11202, https://doi.org/10.1029/2006JD008003, 2007.

Friman, M., Aurela, M., Saarnio, K., Teinilä, K., Kesti, J., Harni, S. D., Saarikoski, S., Hyvärinen, A., and Timonen, H.: Long-term characterization of organic and elemental carbon at three different background areas in northern Europe, Atmos. Environ., 310, https://doi.org/10.1016/j.atmosenv.2023.119953, 2023.

Gensch, I., Kiendler-Scharr, A., and Rudolph, J.: Isotope ratio studies of atmospheric organic compounds: Principles, methods, applications and potential, Int. J. Mass Spectrom., 365–366, 206–221, https://doi.org/10.1016/j.ijms.2014.02.004, 2014.

Groot Zwaaftink, C. D., Grythe, H., Skov, H., and Stohl, A.: Substantial contribution of northern high-latitude sources to mineral dust in the Arctic, J. Geophys. Res., 121, 13678–13697, https://doi.org/10.1002/2016JD025482, 2016.

Gu, W., Xie, Z., Wei, Z., Chen, A., Jiang, B., Yue, F., and Yu, X.: Marine Fresh Carbon Pool Dominates Summer Carbonaceous Aerosols Over Arctic Ocean, J. Geophys. Res.-Atmos., 128, https://doi.org/10.1029/2022JD037692, 2023.

Hasegawa, S.: Experimental Characterization of $PM_{2.5}$ Organic Carbon by Using Carbon-fraction Profiles of Organic Materials, Asian J. Atmos. Environ., 16, 2021128, https://doi.org/10.5572/ajae.2021.128, 2022.

Holtz, L. M., Wolf-Gladrow, D., and Thoms, S.: Stable carbon isotope signals in particulate organic and inorganic carbon of coccolithophores – A numerical model study for Emiliania huxleyi, J. Theor. Biol., 420, 117–127, https://doi.org/10.1016/j.jtbi.2017.01.030, 2017.

Hu, Z., Kang, S., Xu, J., Zhang, C., Li, X., Yan, F., Zhang, Y., Chen, P., and Li, C.: Significant overestimation of black carbon concentration caused by high organic carbon in aerosols of the Tibetan Plateau, Atmos. Environ., 294, 119486, https://doi.org/10.1016/j.atmosenv.2022.119486, 2023.

Huang, L., Brook, J. R., Zhang, W., Li, S. M., Graham, L., Ernst, D., Chivulescu, A., and Lu, G.: Stable isotope measurements of carbon fractions (OC/EC) in airborne particulate: A new dimension for source characterization and apportionment, Atmos. Environ., 40, 2690–2705, https://doi.org/10.1016/j.atmosenv.2005.11.062, 2006.

Huang, L., Zhang, W., Santos, G. M., Rodríguez, B. T., Holden, S. R., Vetro, V., and Czimczik, C. I.: Application of the ECT9 protocol for radiocarbon-based source apportionment of carbonaceous aerosols, Atmos. Meas. Tech., 14, 3481–3500, https://doi.org/10.5194/amt-14-3481-2021, 2021.

Jankowski, N., Schmidl, C., Marr, I. L., Bauer, H., and Puxbaum, H.: Comparison of methods for the quantification of carbonate carbon in atmospheric $PM_{10}$ aerosol samples, Atmos. Environ., 42, 8055–8064, https://doi.org/10.1016/j.atmosenv.2008.06.012, 2008.

Karanasiou, A., Diapouli, E., Cavalli, F., Eleftheriadis, K., Viana, M., Alastuey, A., Querol, X., and Reche, C.: On the quantification of atmospheric carbonate carbon by thermal/optical analysis protocols, Atmos. Meas. Tech., 4, 2409–2419, https://doi.org/10.5194/amt-4-2409-2011, 2011.

Kawai, K., Matsui, H., and Tobo, Y.: Dominant Role of Arctic Dust With High Ice Nucleating Ability in the Arctic Lower Troposphere, Geophys. Res. Lett., 50, https://doi.org/10.1029/2022GL102470, 2023.

Kawamura, K. and Watanabe, T.: Determination of stable carbon isotopic compositions of low molecular weight dicarboxylic acids and ketocarboxylic acids in atmospheric aerosol and snow samples, Anal. Chem., 76, 5762–5768, https://doi.org/10.1021/ac049491m, 2004.

Kawamura, K., Yanase, A., Eguchi, T., Mikami, T., and Barrie, L. A.: Enhanced atmospheric transport of soil derived organic matter in spring over the Arctic, Geophys. Res. Lett., 23, 3735–3738, https://doi.org/10.1029/96GL03537, 1996.

Laskin, A., Laskin, J., and Nizkorodov, S. A.: Chemistry of Atmospheric Brown Carbon, Chem. Rev., 115, 4335–4382, https://doi.org/10.1021/cr5006167, 2015.

Liu, D., He, C., Schwarz, J. P., and Wang, X.: Lifecycle of light-absorbing carbonaceous aerosols in the atmosphere, npj Clim. Atmos. Sci., 3, https://doi.org/10.1038/s41612-020-00145-8, 2020.

Mbengue, S., Zikova, N., Schwarz, J., Vodička, P., Šmejkalová, A. H., and Holoubek, I.: Mass absorption cross-section and absorption enhancement from long term black and elemental carbon measurements: A rural background station in Central Europe, Sci. Total Environ., 794, https://doi.org/10.1016/j.scitotenv.2021.148365, 2021.

McClelland, H. L. O., Bruggeman, J., Hermoso, M., and Rickaby, R. E. M.: The origin of carbon isotope vital effects in coccolith calcite, Nat. Commun., 8, 1–16, https://doi.org/10.1038/ncomms14511, 2017.

Meinander, O., Dagsson-Waldhauserova, P., Amosov, P., Aseyeva, E., Atkins, C., Baklanov, A., Baldo, C., Barr, S. L., Barzycka, B., Benning, L. G., Cvetkovic, B., Enchilik, P., Frolov, D., Gassó,

S., Kandler, K., Kasimov, N., Kavan, J., King, J., Koroleva, T., Krupskaya, V., Kulmala, M., Kusiak, M., Lappalainen, H. K., Laska, M., Lasne, J., Lewandowski, M., Luks, B., McQuaid, J. B., Moroni, B., Murray, B., Möhler, O., Nawrot, A., Nickovic, S., O'Neill, N. T., Pejanovic, G., Popovicheva, O., Ranjbar, K., Romanias, M., Samonova, O., Sanchez-Marroquin, A., Schepanski, K., Semenkov, I., Sharapova, A., Shevnina, E., Shi, Z., Sofiev, M., Thevenet, F., Thorsteinsson, T., Timofeev, M., Umo, N. S., Uppstu, A., Urupina, D., Varga, G., Werner, T., Arnalds, O., and Vukovic Vimic, A.: Newly identified climatically and environmentally significant high-latitude dust sources, Atmos. Chem. Phys., 22, 11889–11930, https://doi.org/10.5194/acp-22-11889-2022, 2022.

Monteiro, F. M., Bach, L. T., Brownlee, C., Bown, P., Rickaby, R. E. M., Poulton, A. J., Tyrrell, T., Beaufort, L., Dutkiewicz, S., Gibbs, S., Gutowska, M. A., Lee, R., Riebesell, U., Young, J., and Ridgwell, A.: Why marine phytoplankton calcify, Sci. Adv., 2, 1–14, https://doi.org/10.1126/sciadv.1501822, 2016.

Moschos, V., Dzepina, K., Bhattu, D., Lamkaddam, H., Casotto, R., Daellenbach, K. R., Canonaco, F., Rai, P., Aas, W., Becagli, S., Calzolai, G., Eleftheriadis, K., Moffett, C. E., Schnelle-Kreis, J., Severi, M., Sharma, S., Skov, H., Vestenius, M., Zhang, W., Hakola, H., Hellén, H., Huang, L., Jaffrezo, J. L., Massling, A., Nøjgaard, J. K., Petäjä, T., Popovicheva, O., Sheesley, R. J., Traversi, R., Yttri, K. E., Schmale, J., Prévôt, A. S. H., Baltensperger, U., and El Haddad, I.: Equal abundance of summertime natural and wintertime anthropogenic Arctic organic aerosols, Nat. Geosci., https://doi.org/10.1038/s41561-021-00891-1, 2022.

Mukherjee, P., Reinfelder, J. R., and Gao, Y.: Enrichment of calcium in sea spray aerosol in the Arctic summer atmosphere, Mar. Chem., 227, 103898, https://doi.org/10.1016/j.marchem.2020.103898, 2020.

Muller, A., Lamb, E. G., and Siciliano, S. D.: The silent carbon pool: Cryoturbic enriched organic matter in Canadian High Arctic semi-deserts, Geoderma, 415, 115781, https://doi.org/10.1016/j.geoderma.2022.115781, 2022.

Narukawa, M., Kawamura, K., Li, S.-M., and Bottenheim, J. W.: Stable carbon isotopic ratios and ionic composition of the high-Arctic aerosols: An increase in $\delta^{13}C$ values from winter to spring, J. Geophys. Res., 113, D02312, https://doi.org/10.1029/2007JD008755, 2008.

Not, C. and Hillaire-Marcel, C.: Enhanced sea-ice export from the Arctic during the Younger Dryas, Nat. Commun., 3, 645–647, https://doi.org/10.1038/ncomms1658, 2012.

Okada, H. and Honjo, S.: Distribution of Oceanic Coccolithophorids in the Pacific., Deep Sea Res., 20, 355–374, https://doi.org/10.1016/0011-7471(73)90059-4, 1973.

Petit, J. E., Favez, O., Albinet, A., and Canonaco, F.: A user-friendly tool for comprehensive evaluation of the geographical origins of atmospheric pollution: Wind and trajectory analyses, Environ. Modell. Softw., 88, 183–187, https://doi.org/10.1016/j.envsoft.2016.11.022, 2017.

Petzold, A., Ogren, J. A., Fiebig, M., Laj, P., Li, S.-M., Baltensperger, U., Holzer-Popp, T., Kinne, S., Pappalardo, G., Sugimoto, N., Wehrli, C., Wiedensohler, A., and Zhang, X.-Y.: Recommendations for reporting "black carbon" measurements, Atmos. Chem. Phys., 13, 8365–8379, https://doi.org/10.5194/acp-13-8365-2013, 2013.

Phillips, R. L. and Grantz, A.: Regional variations in provenance and abundance of ice-rafted clasts in Arctic Ocean sediments: Implications for the configuration of late Quaternary oceanic and atmospheric circulation in the Arctic, Mar. Geol., 172, 91–115, https://doi.org/10.1016/S0025-3227(00)00101-8, 2001.

Pushkareva, E., Johansen, J. R., and Elster, J.: A review of the ecology, ecophysiology and biodiversity of microalgae in Arctic soil crusts, Polar Biol., 39, 2227–2240, https://doi.org/10.1007/s00300-016-1902-5, 2016.

Raman, R. S., Ramachandran, S., and Kedia, S.: A methodology to estimate source-specific aerosol radiative forcing, J. Aerosol Sci., 42, 305–320, https://doi.org/10.1016/j.jaerosci.2011.01.008, 2011.

Rodríguez, B. T., Huang, L., Santos, G. M., Zhang, W., Vetro, V., Xu, X., Kim, S., and Czimczik, C. I.: Seasonal Cycle of Isotope-Based Source Apportionment of Elemental Carbon in Airborne Particulate Matter and Snow at Alert, Canada, J. Geophys. Res.-Atmos., 125, https://doi.org/10.1029/2020JD033125, 2020.

Savadkoohi, M., Pandolfi, M., Favez, O., Putaud, J. P., Eleftheriadis, K., Fiebig, M., Hopke, P. K., Laj, P., Wiedensohler, A., Alados-Arboledas, L., Bastian, S., Chazeau, B., María, Á. C., Colombi, C., Costabile, F., Green, D. C., Hueglin, C., Liakakou, E., Luoma, K., Listrani, S., Mihalopoulos, N., Marchand, N., Močnik, G., Niemi, J. V., Ondráček, J., Petit, J. E., Rattigan, O. V., Reche, C., Timonen, H., Titos, G., Tremper, A. H., Vratolis, S., Vodička, P., Funes, E. Y., Zíková, N., Harrison, R. M., Petäjä, T., Alastuey, A., and Querol, X.: Recommendations for reporting equivalent black carbon (eBC) mass concentrations based on long-term pan-European in-situ observations, Environ. Int., 185, 108553, https://doi.org/10.1016/j.envint.2024.108553, 2024.

Sharma, S., Lavoué, D., Chachier, H., Barrie, L. A., and Gong, S. L.: Long-term trends of the black carbon concentrations in the Canadian Arctic, J. Geophys. Res.-Atmos., 109, https://doi.org/10.1029/2003JD004331, 2004.

Sharma, S., Leaitch, W. R., Huang, L., Veber, D., Kolonjari, F., Zhang, W., Hanna, S. J., Bertram, A. K., and Ogren, J. A.: An evaluation of three methods for measuring black carbon in Alert, Canada, Atmos. Chem. Phys., 17, 15225–15243, https://doi.org/10.5194/acp-17-15225-2017, 2017.

Sharma, S., Barrie, L. A., Magnusson, E., Brattström, G., Leaitch, W. R., Steffen, A., and Landsberger, S.: A Factor and Trends Analysis of Multidecadal Lower Tropospheric Observations of Arctic Aerosol Composition, Black Carbon, Ozone, and Mercury at Alert, Canada, J. Geophys. Res.-Atmos., 124, 14133–14161, https://doi.org/10.1029/2019JD030844, 2019.

Sirois, A. and Barrie, L. A.: Arctic lower tropospheric aerosol trends and composition at Alert, Canada: 1980–1995, J. Geophys. Res., 104, 11599–11618, 1999.

Smith, H. E. K., Tyrrell, T., Charalampopoulou, A., Dumousseaud, C., Legge, O. J., Birchenough, S., Pettit, L. R., Garley, R., Hartman, S. E., Hartman, M. C., Sagoo, N., Daniels, C. J., Achterberg, E. P., and Hydes, D. J.: Predominance of heavily calcified coccolithophores at low $CaCO_3$ saturation during winter in the Bay of Biscay, P. Natl. Acad. Sci. USA, 109, 8845–8849, https://doi.org/10.1073/pnas.1117508109, 2012.

Stein, A. F., Draxler, R. R., Rolph, G. D., Stunder, B. J. B., Cohen, M. D., and Ngan, F.: NOAA's HYSPLIT atmospheric transport and dispersion modeling system, B. Am. Meteo-

rol. Soc., 96, 2059–2077, https://doi.org/10.1175/BAMS-D-14-00110.1, 2015.

Stein, R., Grobe, H., and Wahsner, M.: Organic carbon, carbonate, and clay mineral distributions in eastern central Arctic Ocean surface sediments, Mar. Geol., 119, 269–285, https://doi.org/10.1016/0025-3227(94)90185-6, 1994.

Stjern, C. W., Samset, B. H., Myhre, G., Bian, H., Chin, M., Davila, Y., Dentener, F., Emmons, L., Flemming, J., Haslerud, A. S., Henze, D., Jonson, J. E., Kucsera, T., Lund, M. T., Schulz, M., Sudo, K., Takemura, T., and Tilmes, S.: Global and regional radiative forcing from 20 % reductions in BC, OC and $SO_4$ – an HTAP2 multi-model study, Atmos. Chem. Phys., 16, 13579–13599, https://doi.org/10.5194/acp-16-13579-2016, 2016.

Toom-Sauntry, D. and Barrie, L. A.: Chemical composition of snowfall in the high Arctic: 1990-1994, Atmos. Environ., 36, 2683–2693, https://doi.org/10.1016/S1352-2310(02)00115-2, 2002.

Verwega, M.-T., Somes, C. J., Schartau, M., Tuerena, R. E., Lorrain, A., Oschlies, A., and Slawig, T.: Description of a global marine particulate organic carbon-13 isotope data set, Earth Syst. Sci. Data, 13, 4861–4880, https://doi.org/10.5194/essd-13-4861-2021, 2021.

Vodička, P.: Carbonate content and stable isotopic composition of atmospheric aerosol carbon in the Canadian High Arctic, Zenodo [data set], https://doi.org/10.5281/zenodo.16994150, 2025.

Vodička, P., Kawamura, K., Schwarz, J., and Ždímal, V.: Seasonal changes in stable carbon isotopic composition in the bulk aerosol and gas phases at a suburban site in Prague, Sci. Total Environ., 803, 149767, https://doi.org/10.1016/j.scitotenv.2021.149767, 2022.

Wang, H. and Kawamura, K.: Stable carbon isotopic composition of low-molecular-weight dicarboxylic acids and ketoacids in remote marine aerosols, J. Geophys. Res.-Atmos., 111, https://doi.org/10.1029/2005JD006466, 2006.

Winiger, P., Barrett, T. E., Sheesley, R. J., Huang, L., Sharma, S., Barrie, L. A., Yttri, K. E., Evangeliou, N., Eckhardt, S., Stohl, A., Klimont, Z., Heyes, C., Semiletov, I. P., Dudarev, O. V., Charkin, A., Shakhova, N., Holmstrand, H., Andersson, A., and Gustafsson: Source apportionment of circum-Arctic atmospheric black carbon from isotopes and modeling, Sci. Adv., 5, 1–10, https://doi.org/10.1126/sciadv.aau8052, 2019.

Zeebe, R. E.: History of seawater carbonate chemistry, atmospheric CO2, and ocean acidification, Annu. Rev. Earth Pl. Sc., 40, 141–165, https://doi.org/10.1146/annurev-earth-042711-105521, 2012.